Macromolecules

Article

pubs.acs.org/Macromolecules

Nanorod Diffusion in Polymer Nanocomposites by Molecular Dynamics Simulations

Argyrios Karatrantos,[†] Russell J. Composto,[‡] Karen I. Winey,[‡] and Nigel Clarke*[,§]

[†]Materials Research and Technology, Luxembourg Institute of Science and Technology, 5, Avenue des Hauts-Fourneaux, L-4362 Esch-sur-Alzette, Luxembourg

[‡]Department of Materials Science and Engineering, University of Pennsylvania, Philadelphia, Pennsylvania 19104, United States

[§]Department of Physics and Astronomy, University of Sheffield, Sheffield S3 7RH, United Kingdom

Supporting Information

ABSTRACT: Nanorod diffusion and polymer dynamics in nanocomposites were investigated by means of molecular dynamics simulations. We show that thin nanorods (spherocylinders) can diffuse much faster than that predicted by a Stokes−Einstein continuum model, similar to experiments, in the dilute nanorod regime. In entangled polymer matrices, nanorod diffusion reaches a plateau region. Increase of the nanorod diameter or aspect ratio (AR) slows its diffusion. The nanorod diffusion regime, at long time scales, displays a non-Gaussian behavior as is depicted by the several Gaussian peaks present in the self-part of the van Hove function. We also show that the unentangled polymer dynamics decreases in the nanocomposite due to the nanorod's interfacial area.

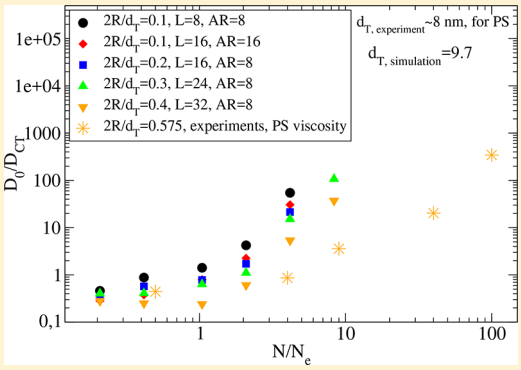

I. INTRODUCTION

The dispersion of spherical nanoparticles or anisotropic nanorods (NRs) into a dense polymer matrix can enhance the mechanical,[1,2] electrical, optical,[3] and plasmonic[4] properties of the materials. There are different diffusion regimes of the nanoparticles into a polymer matrix which can be distinguished by calculating the mean-square displacement (MSD) of the nanoparticles as a function of time.[5] On very short time scales, there is a ballistic motion of the nanoparticles where MSD $\sim t^2$.[6] Beyond that regime, there is subdiffusion motion of the nanoparticles where MSD $\sim t^{0.5}$, while at longer times the nanoparticles follow a Fickian diffusive motion where MSD $\sim t^1$. The theory of Stokes−Einstein predicts the Brownian diffusive motion of (nano)particles[7] in a viscous medium (either polymer matrix or solvent). In the case of NRs in a medium, the Stokes−Einstein equation can be modified[8] to predict their Brownian diffusive motion in a dilute nanorod regime. Such a continuum model predicts a decrease of the nanorod diffusion with molecular weight of the matrix (M). However, if the nanorod's diameter D is smaller than the tube diameter of the polymer matrix, d_T, diffusion does not follow the Stokes−Einstein modified formula according to experiments.[9,10] This is also the case for spherical nanoparticles into a polymer matrix.[11−22] In particular, by use of Rutherford backscattering spectrometry, the diffusion of titanium dioxide (TiO_2) nanorods (of length L = 43 nm, diameter D = 5 nm, and aspect ratio AR ≈ 9) was measured in a polystyrene matrix (the molecular weights (M) of the matrix range from 9 to 2000 kDa, D/d_T = 0.51−0.575).[10] In the entangled polymer matrix, the diffusion coefficients (D) of TiO_2 nanorods[10] decreases as $M^{-1.4}$, whereas the Stokes−Einstein continuum model (CM) predicts a M^{-3} dependence due to the molecular weight dependence of matrix viscosity. Thus, TiO_2 nanorod diffusion in PS melts is faster than that predicted by the Stokes−Einstein continuum model. In contrast, the theory of de Gennes and Wyart[23,24] predicted that nanorod's motion does not depend on polymer molecular weight.

In a recent study, the mobility of gold nanorods within entangled wormlike micelle solution[25] was investigated by X-ray photon correlation (XPCS) spectroscopy. It was found that on short time scales, which cannot be captured by XPCS measurements, the nanorod motion is restricted to a localization length, which is controlled by the elasticity of the entangled micelles following the Stokes−Einstein relation when the nanorod length is larger than the entanglement mesh. On long time scales the nanorods diffuse with a diffusivity that exceeds the Stokes−Einstein prediction following a "hopping" nanoparticle mechanism similar to the one observed in entangled polymer solutions.[5,26−29] In addition, the translational and the rotational dynamics of a single thin gold nanorod in solution have been studied recently by experiments[30] and by coarse-grained simulations.[31,32] These two types of dynamics are decoupled in unentangled polymer matrices.[31] In another experimental study, multiple nanorods

Received: October 8, 2018
Revised: January 25, 2019

DOI: 10.1021/acs.macromol.8b02141
Macromolecules XXXX, XXX, XXX−XXX

of certain diameter and concentration have been studied in solutions.[33] By use of birefringence,[34] it was shown that the orientational nanocelluloses dynamics depends on the polydispersity of the nanorods. A non-Gaussian dynamics (hopping) has also been observed in experimental systems of polystyrene (PS) NPs in poly(ethylene oxide) (PEO) solutions,[35] gold NPS in entangled poly(vinyl alcohol) solutions,[29] and quantum dot NPs in polyacrylamide gels[36] in coarse-grained models of polymer melt with spherical nanoparticles[18,37−39] and hard sphere fluid.[40]

To the best of our knowledge there is not any simulation work that mimics a nanocomposite[41] (or suspension) containing nanorods at a finite nanorod loading and investigates the nanorod diffusion in a polymer matrix in comparison to theory and experiments. In this article we explore how thin nanorods (the nanorod diameter, D, is smaller the polymer radius of gyration, R_g[42−44]) diffuse in dense polymer melts in comparison to experiments.[10] The rest of this paper is organized as follows. In section II the simulation methodology and details are described. In section A the structure of the nanorods inside unentangled and entangled polymer matrices is investigated. In section B, nanorod diffusion (and its mechanism) in both unentangled and entangled polymer matrices is calculated, at dilute nanorod loading, and compared to the Stokes−Einstein continuum model and experiments. Subsequently, in section C the unentangled polymer dynamics is investigated. Finally, in section IV conclusions are presented.

II. SIMULATION METHODOLOGY

Stochastic molecular dynamics simulations were implemented by using the GROMACS 4.5.3 package.[19,45−48] In particular, the Newton−Langevin equations were solved:[45,49]

$$m_i \frac{d\mathbf{v}_i}{dt} = -\nabla V_i - \Gamma \frac{d\mathbf{r}_i}{dt} + \mathbf{W}_i(t) \tag{1}$$

where V_i is the total potential experienced by particle i which is a sum of three terms:

$$V_i = \sum_{j \neq i} (V_{ij}^{LJ} + V_{ij}^{S} + V_{ijk}^{B}) \tag{2}$$

A particle i has mass m_i; Γ is the friction coefficient, and $\mathbf{W}_i$ is a random force. The total force $\mathbf{f}_i$ on particle i is the gradient of the V_i. The monomers of the polymer chain were connected using the FENE potential:[49]

$$V_{ij}^{S} = -\frac{1}{2} k R_0^2 \ln\left(1 - \frac{r^2}{R_0^2}\right) \tag{3}$$

The equilibrium bond length was set to $R_0 = 1.5$ and $k = 30$.[49] We incorporated an intrinsic stiffness into the Kremer−Grest model[49] through a harmonic potential[50] of the following form:

$$V_{ijk}^{B} = \frac{1}{2} k_\theta (\cos\theta_{ijk} - \cos\theta_0)^2 \tag{4}$$

An equilibrium bending angle between three consecutive monomers, $\theta_0 = 109.5°$, with a bending force constant $k_\theta = 25$[50] was used. This polymer model results in an entanglement length $N_e \approx 48$ (from the S-coil estimator[39,51]) and polymer tube diameter $d_T \approx 9.7\sigma_m$ using the geometrical analysis method (Z1 code).[52] The nanocomposite systems contain nanorods (spherocylinders as depicted in Figure 1) which are dispersed in a dense polymer matrix. For the nanorod

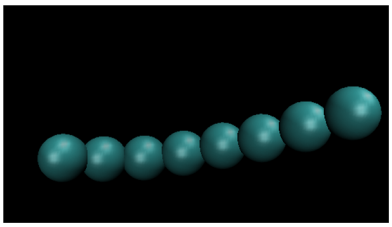

Figure 1. Picture of a spherocylinder nanorod with aspect ratio AR = 8 that is used in our study.

(spherocylinder), the relation $V_{ijk}^{B} = \frac{1}{2} k_\theta (\theta_{ijk} - \theta_0)^2$ is used along three spheres of the nanorod where $\theta_0 = 180°$ and $k_\theta = 50$. The spheres of the nanorod are connected by the potential of the form $V_{ij}^{S} = \frac{1}{2} k_0 (r_{ij} - D)^2$, where $k_0 = 1111.2$.

The Lennard-Jones (LJ) potential V_{ij}^{LJ} which acts between the centers of mass of two particles[53] is

$$V_{ij}^{LJ} = 4\epsilon_{ij}\left(\frac{\sigma^{12}}{r_{ij}^{12}} - \frac{\sigma^6}{r_{ij}^6}\right) \tag{5}$$

where r_{ij} is the distance between particles i and j, ϵ_{ij} is the interaction between particles i and j (specifically, for monomers: $\epsilon_m = \sigma_m = m_m = 1$; for nanorods: $\epsilon_p = 1$, $D = 2R$, $2R/\sigma_m = 1$−4, $m_p = 0.85\frac{4}{3}\pi R^3$). For monomer (m)−nanorod (p) interactions the combination rules $\epsilon_{mp} = (\epsilon_m \epsilon_p)^{1/2}$ and $\sigma_{mp} = (\sigma_m + D)/2$[53] were used. The monomers (or nanorods) are modeled with the repulsive-only part of eq 5, shifted, and truncated at cutoff radius at $r_c = 2^{1/6}\sigma_m$ ($r_c = 2^{1/6}\sigma_p$ for nanorods). However, for the monomer−nanorod interaction, the cutoff radius of the LJ potential (eq 5) is $r_c = 2.4\sigma_{mp}$. The nonbonded intramolecular interaction between the spheres of the nanorods is excluded. The total number of monomers in the cubic simulation cell was either $N_t = 23600$ or 47200 containing nanorods of diameter $D = 1$, 2, 3, or 4. The simulated nanorod volume fraction ϕ is defined as $\phi = \frac{\pi D^2 L N_n}{6\langle V\rangle} \approx 5\%$ (dilute nanorod loading that jamming does not occur[10]), where $\langle V\rangle$ is the average volume of the nanocomposite simulation box in the NPT ensemble. In nanocomposites, the starting structures were created by an ensemble of polymers with $N = 200$ (or $N = 400$) and nanorods inserted at random positions within a large simulation box. For equilibration, the fast push-off method was applied.[54] The pressure calculated for the $N = 200$ polymer melt was $P^* = P\sigma_m^3/\epsilon_m = 4.864$ and was used to perform the simulations of the nanocomposites in the NPT ensemble. The R_g had reached a constant value with time. All the polymers have a Gaussian conformation;[55] the ratio $\langle R_{ee}\rangle^2/\langle R_{ee}\rangle^2 \approx 6.0$−6.1 (the mean-square internal distances are shown in the Supporting Information). Details of the nanocomposites modeled are given in Table 1. A snapshot of a nanocomposite sample is depicted in Figure 2.

Table 1. Nanorod Volume Fraction ϕ (%), Number of Nanorods N_n, and Diameter of Nanorods D (Measured in Units of the Monomer Size σ_m)

ϕ (%)	N_n $D = 1$ (AR = 16)	N_n $D = 2$ (AR = 8)	N_n $D = 4$ (AR = 5)	N_n $D = 3$ (AR = 8)	N_n $D = 4$ (AR = 8)
5	400	100	23	15	15

DOI: 10.1021/acs.macromol.8b02141
Macromolecules XXXX, XXX, XXX−XXX

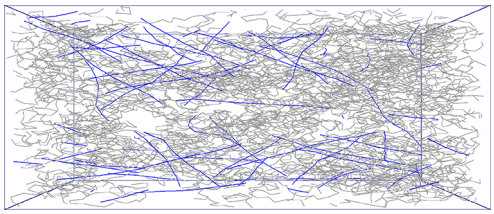

Figure 2. Polymer matrix with chains shown in gray and dispersed nanorods shown in blue.

The length of the simulation cell was larger than the end-to-end distance of the polymers, and it was confirmed that the polymers do not interact with its periodic image. The Langevin thermostat[46] was used to set the temperature at $T = k_B T/\epsilon = 1$, with a friction constant $\Gamma = 0.5\tau^{-1}$.[19,56] As a reference, the glass transition (T_g) of a polymer model that contains a bending potential (but not a torsional potential) is $T_g = 0.4$.[50] The Berendsen barostat was used, with time constant $\tau_p = 2\tau$, to set pressure at $P^* = 4.864$. The equations of motion were integrated using the leapfrog algorithm[57] with a time step $dt = 0.004\tau$, where τ is the Lennard-Jones time.

In the next sections we investigate the effect of nanorod diameter, aspect ratio, and polymer matrix on nanorod diffusion and polymer dynamics.

III. RESULTS AND DISCUSSION

A. Nanorod Structure. In this section we investigate the dispersion of the nanorods[58−63] into unentangled and entangled polymer matrices in the dilute nanorod regime (ϕ = 5%). The nanorod dispersion[64−66] in a polymer matrix depends on the polymer−nanorod interaction, and the best dispersion state can be achieved at an intermediate interphasial interaction.[67,68] First we show in Figure 3 the intermolecular

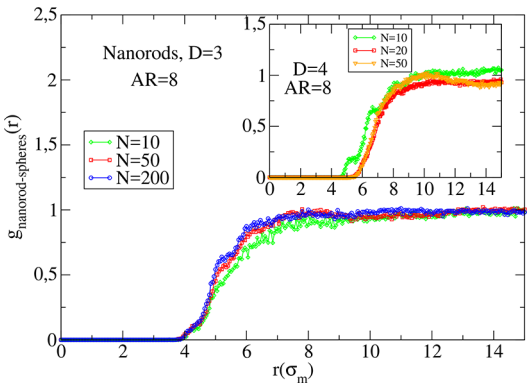

Figure 3. Radial distribution function between the spheres of different nanorods in the polymer matrix.

nanorod−nanorod radial distribution function (RDF) (between the spheres of the nanorod) of nanorods with diameter $D = 3$ and AR = 8. (Similar behavior appears for nanorods of the other nanocomposites studied, as is depicted in the inset of Figure 3 for $D = 4$ and AR = 8.) It can been seen that there is no peak with a value higher than the bulk value which appears at a distance of $r \approx 8$. The monomer−nanorod RDF $g_{mp}(r)$ exhibits a layering structure as is depicted in Figure 4. There is a high monomer density around the nanorod which establish a well-defined interface between nanorods and polymers. The first peak of RDF in Figure 4 appears at contact distance

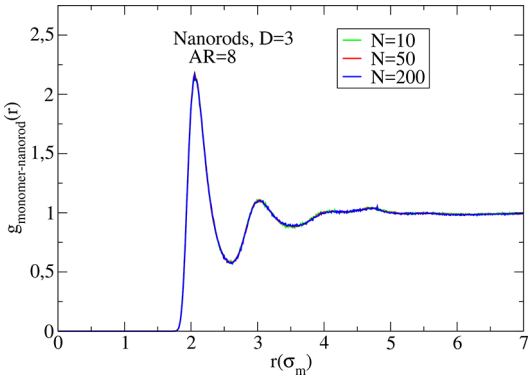

Figure 4. Radial distribution function between the monomers of the polymers and spheres of the nanorods.

between monomers and polymers which is $r = \frac{D+\sigma_m}{2}$. The matrix length does not show any effect on the monomer density around the nanorod. It has been seen that there is no change in the polymer primitive path by the addition of ≈10% nanorod loading.[69]

B. Nanorod Diffusion. The diffusion of nanorods in a medium can be predicted by a Stokes−Einstein (SE) continuum model.[8] The diffusion coefficient D_{CT} of the nanorod of diameter D in a fluid of viscosity η is given by[7,8,68]

$$D_{CT} = \frac{T^*}{3\pi\eta^* L^*} \ln(L^*/D^*) \tag{6}$$

where $\eta^* = \frac{\eta\sigma_m^3}{k_B T\tau}$ is the viscosity of the polymer matrix, $D^* = D/\sigma_m$, and $L^* = L/\sigma_m$. The simulated viscosities of the polymer melts are given by ref 70 and for long polymers (N = 200, 400) by ref 71. The nanorod diffusivity can be calculated from the mean-square displacement (MSD) measurements of the beads of the spherocylinder[72] and is given by

$$D_0 = \frac{1}{6}\lim_{t\to\infty}\frac{d}{dt}\langle|\mathbf{r}_i(t) - \mathbf{r}_i(0)|^2\rangle \tag{7}$$

where $\langle|\mathbf{r}_i(t) - \mathbf{r}_i(0)|^2\rangle$ is the time-dependent displacement of the beads of spherocylinder averaged over time and particles of the ensemble ($\mathbf{r}_i$ is the position of a particle i).

The diffusion of thin nanorods reaches a plateau for $N \geq 100$ (entangled polymer matrices), as depicted in Figure 5, in agreement with the GLE theory[12,15] and by de Gennes,[24,73] who claimed that bulk viscosity does not capture the behavior of the medium near nanoparticles, and thus the nanoparticles diffusion is decoupled from the SE formula (eq 6). Because the nanorod diameter is smaller than the entanglement mesh, the nanorods can diffuse faster in comparison to the SE theoretical predictions due to local viscosity.[15,74,75] A qualitative similar plateau regime in entangled matrices appears for spherical nanoparticles, where nanoparticle diffusivity approaches the Stokes−Einstein predictions when the diameter of the nanoparticle is approximately 2−3 times the matrix tube diameter, as was evidenced in poly(n-butyl methacrylate)/gold composites,[76,77] fullerene/polystyrene composites,[78] and theoretical studies.[74,79,80] However, in entangled poly(2-vinylpyridine) (P2VP)/nanosilica composites (where attractive polymer−nanoparticle interactions are present), nanosilica diffusion in P2VP is well-described by the Stokes−Einstein formula, since $2R/d_T = 3$. In addition, the diffusivity of the

DOI: 10.1021/acs.macromol.8b02141
Macromolecules XXXX, XXX, XXX−XXX

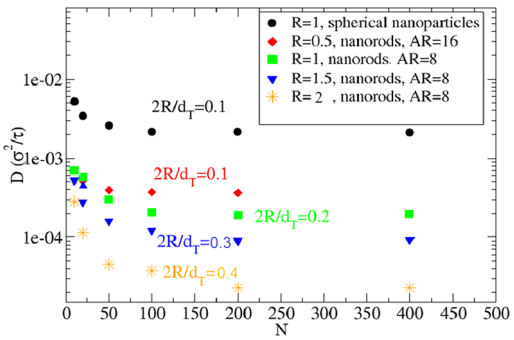

Figure 5. Dependence of nanorods diffusivity in unentangled and entangled polymer matrices of different diameter: spherical nanoparticles of diameter $D = 2$ (circles),[19] nanorods of $D = 1$, AR = 16 (diamonds), nanorods of $D = 2$, AR = 8 (squares), nanorods $D = 3$, AR = 8 (down triangles), nanorods of $D = 4$, AR = 8 (stars). Tube diameter of polymer model: $d_T = 9.7\sigma_m$. Tube diameter of PS: $d_T = 8$ nm.

nanorods decreases with AR as is depicted in Figure 5 for $2R/d_T = 0.1$.

We show in Figure 6 the nanorod diffusivity in different polymer matrices, scaled with the theoretical predictions (eq 6). In the dilute nanorod regime ($\phi = 5\%$) thin nanorods ($D = 2$) diffuse faster than the SE prediction[15] for matrices $N \geq 50$ ($N/N_e > 1$). In nanocomposites containing an unentangled polymer matrix simulation data agree with experiments.[10] It can be seen that such nanorods, thinner than the tube diameter d_T ($d_T \approx 9.7\sigma_m$ for our polymer model), deviate more from the SE predictions with increasing M. The discrepancy is larger for entangled polymer matrices due to the viscosity scaling with molecular weight $\eta \propto N^{3.4}$ in the entangled regime.

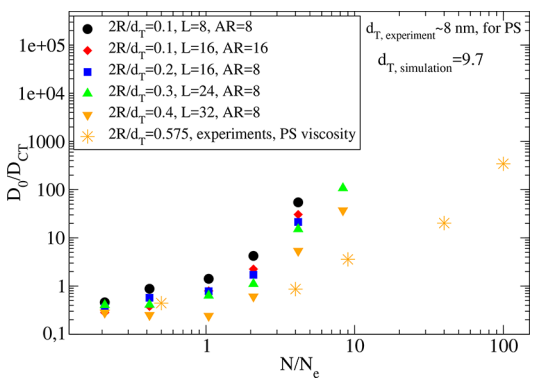

Figure 6. Dependence of scaled nanorods diffusivity in unentangled and entangled polymer matrices for different nanorod diameters: spherical nanoparticles of diameter, $D = 2$ (circles),[19] nanorods of $D = 1$, AR = 16 (diamonds), nanorods of $D = 2$, AR = 8 (squares), nanorods $D = 3$, AR = 8 (down triangles), nanorods of $D = 4$, AR = 8 (stars), experiments (stars).[10]

Nanorod diffusivity decreases, as can be seen in the Figure 5, if D increases and the scaled diffusivity value approaches more the experimental data as is depicted in Figure 6. The discrepancy between the simulation and experimental data in the entangled polymer matrices might come from the thinner nanorods that were used in the simulations. It has been shown by simulations[22] that nanoparticles of diameter $D \geq d_T$ do not follow the plateau diffusivity regime in entangled polymer matrices, but its diffusivity rather decreases with polymer molecular weight.

Furthermore, we calculated the displacement distribution of the nanorods at different times by obtaining the self-part of the van Hove function (VHF)

$$G_s(r, \Delta t) = \langle \delta[r - |\mathbf{r}_i(t_0 + \Delta t) - \mathbf{r}_i(t_0)|] \rangle_{t_0} \quad (8)$$

which gives the probability distribution to find a nanoparticle at a distance r from the initial position (at time t_0) after a time interval Δt. The probability is normalized as $\int G_s(r,\Delta t)\, d^3r = 1$. As can be seen from Figure 7, at small time intervals 3000τ and 15000τ, the data can be fitted to a single Gaussian function (eq 9) with a peak value corresponding to the most probable traveled distance during that time interval Δt. However, at long time scales (diffusive regime) a bimodal function is necessary to model the displacement of the nanoparticles in the polymer matrix. Moreover, for thinner rods of $D = 1$ (or $D = 2$), even at short time scales of 3000τ, a non-Gaussian dynamics is presented as can be seen in Figure 7d−f (see also Figure S9). This denotes a hopping fashion of motion of the nanorods (similar behavior of the van Hove functions in other nanocomposite systems is shown in the Supporting Information).

$$G_s(r, \Delta t) = (4\pi D\Delta t)^{-3/2} e^{-r^2/4D\Delta t} \quad (9)$$

In previous simulation studies (both atomistic[6,81] and coarse grained[37−39]) it was shown that even small nanoparticles (such as fullerene) smaller than the entanglement mesh can follow a hopping type of motion in a polymer matrix.

C. Polymer Dynamics. In polymer−nanorod composites,[82] the nanorods act as extra entanglements[83] that can alter the polymer primitive path[83−85] and thus the polymer dynamics.[9] It has been observed that in nanocomposites that contain attractive polymer/nanoparticle interaction, such as nanosilica/poly(ethylene glycol) (PEO) or poly(butylene oxide) (PBO) mixtures,[86] polymer dynamics is affected by the nanoparticles,[87] especially in nanoparticle loading larger than the dilute regime ($\phi = 5\%$). By increasing the nanorods loading in the matrix, the interphase around the nanorods would increase since more monomers exist into the interphasial area.[88] Figure 8 shows the mean-square displacement (MSD) of unentangled polymers in melts and nanocomposites containing different nanorods. It can be seen that on long time scales the polymer dynamics (diffusion) is lower in nanocomposites. The discrepancy in the polymer MSD between melts and nanocomposites is higher for the oligomers ($N = 10, 20$) due to more monomers that are in contact with nanorod surface. Recently, it was shown in experiments that tracer (polymer) diffusion can be enhanced by the mobility of nanorods relative to the case of immobile nanorods.[89] In addition, in nanocomposites containing nanosilicas (tethered with poly(ethylene glycol) chains) in a poly(methyl methacrylate) (PMMA) matrix, PMMA dynamics undergoes a continuous transition from a bulklike behavior at low loading to a confinement behavior at intermediate loading and eventually to glassy behavior at high loading.[90] The mechanism of polymer diffusion reduction in those experimental and our simulation data is due to nanoparticle interfacial area[88,91,92] and not due to entropic barriers.

DOI: 10.1021/acs.macromol.8b02141
Macromolecules XXXX, XXX, XXX−XXX

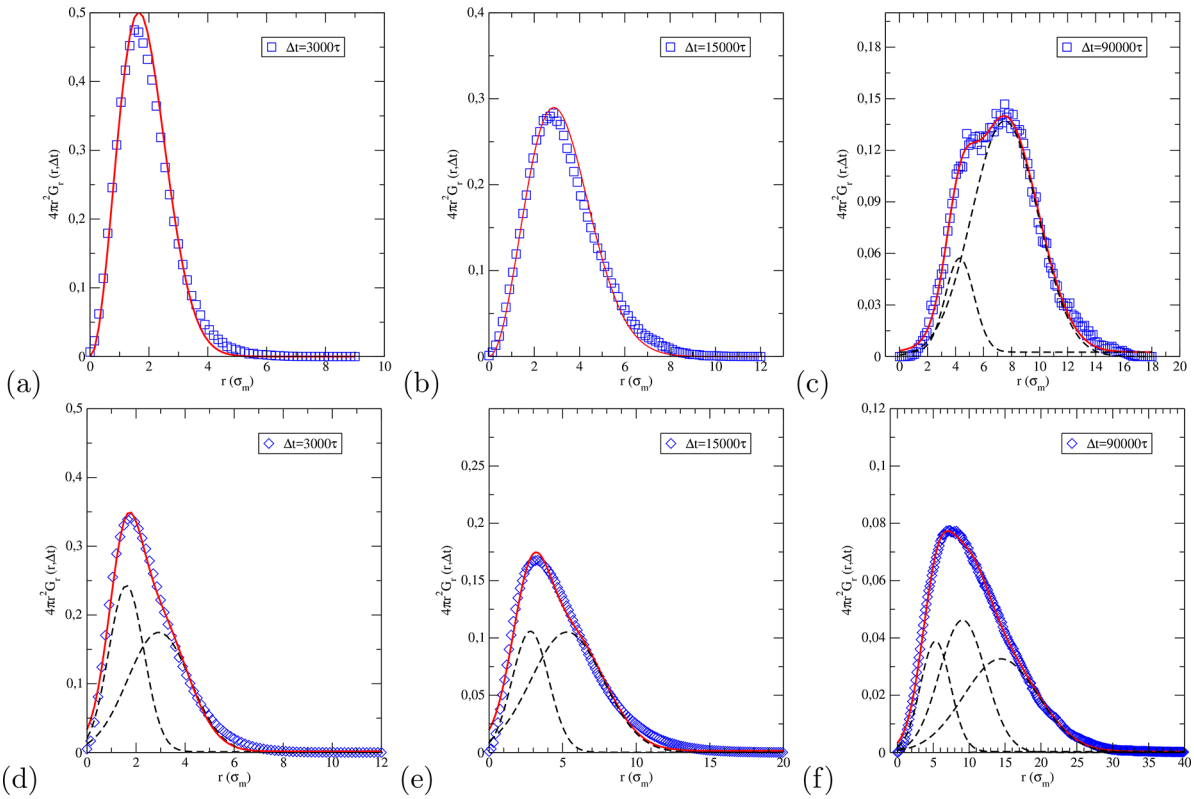

Figure 7. van Hove function $G_s(r,\Delta t)$ for nanorods in nanocomposite, nanorod diameter D = 3, AR = 8, polymer matrix N = 200 (blue squares), nanorod diameter D = 1, AR = 16, polymer matrix N = 200 (blue diamonds) at three different Δt. Symbols are simulation data and solid lines are fitting of eq 7 in the first two panels (a) + (b) for $\Delta t \leq 15\tau$, while the right panel (d) for larger time interval $\Delta t = 90\tau$ can only be fitted by a superposition of two Gaussians. The individual contributions are shown by black dashed lines.

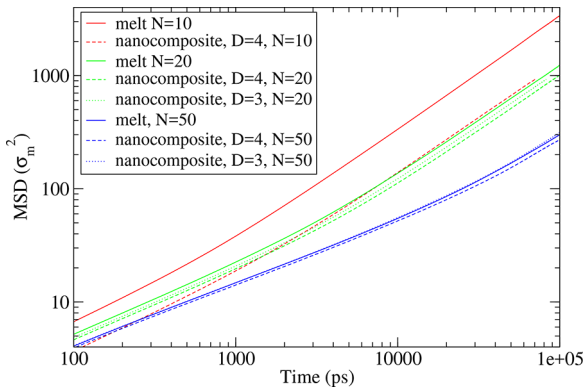

Figure 8. Polymers mean-square displacement of different molecular weights. Solid lines: melts; dashed lines: nanocomposites of D = 4, AR = 8; dotted lines: nanocomposites of D = 3, AR = 8.

IV. CONCLUSIONS

Nanorod diffusion and polymer dynamics in nanocomposites were investigated by means of coarse-grained molecular dynamics simulations. We showed that thin nanorods can diffuse faster than the prediction of the Stokes−Einstein continuum model in entangled matrices. The simulated data predict the nanorod diffusion in agreement with experiments in unentangled matrices but overpredict the nanorod diffusion in entangled polymer matrices. The nanorods follow a hopping type of motion in the polymer matrix. In addition, we have found that nanorods hinder polymer chains motion, even at a dilute nanorod loading.

■ ASSOCIATED CONTENT

Supporting Information

The Supporting Information is available free of charge on the ACS Publications website at DOI: 10.1021/acs.macromol.8b02141.

Figures S1−S15 (PDF)

■ AUTHOR INFORMATION

Corresponding Author

*E-mail n.clarke@sheffield.ac.uk.

ORCID

Argyrios Karatrantos: 0000-0002-3169-6894

Russell J. Composto: 0000-0002-5906-2594

Karen I. Winey: 0000-0001-5856-3410

Notes

The authors declare no competing financial interest.

■ ACKNOWLEDGMENTS

This research was funded by the EPSRC/NSF Materials Network Program Nos. EP/5065373/1 (EPSRC: N.C. and A.K.) and DMR-1210379 (NSF: K.I.W. and R.J.C.). Support was also provided by ACS/PRF 54028-ND7 (R.J.C.) and NSF/DMR 1507713 (R.J.C.).We appreciate the computational time in Iceberg HPC of the University of Sheffield.

■ REFERENCES

(1) Buxton, G. A.; Balazs, A. C. Predicting the mechanical and electrical properties of nanocomposites formed from polymer blends and nanorods. *Mol. Simul.* **2004**, *30*, 249−257.

DOI: 10.1021/acs.macromol.8b02141
Macromolecules XXXX, XXX, XXX−XXX

(2) Tang, L.; Weder, C. Cellulose whisker/epoxy resin nanocomposites. *ACS Appl. Mater. Interfaces* **2010**, *2*, 1073−1080.
(3) Hore, M. J. A.; Frischknecht, A. L.; Composto, R. J. Nanorod assemblies in polymer films and their dispersion-dependent optical properties. *ACS Macro Lett.* **2012**, *1*, 115−121.
(4) Ferrier, R. C.; Hyun-Su Lee, M. J; Hore, A.; Caporizzo, M.; Eckmann, D. M.; Composto, R. J. Gold nanorod linking to control plasmonic properties in solution and polymer nanocomposites. *Langmuir* **2014**, *30*, 1906−1914.
(5) Cai, L. H.; Panyukov, S.; Rubinstein, M. Mobility of nonsticky nanoparticles in polymer liquids. *Macromolecules* **2011**, *44*, 7853.
(6) Volgin, I. G.; Larin, S. V.; Abad, E.; Lyulin, S. V. Molecular dynamics simulations of fullerene diffusion in polymer melts. *Macromolecules* **2017**, *50*, 2207−2218.
(7) Einstein, A. Eine neue bestimmung der molekldimensionen. *Ann. Phys. (Berlin, Ger.)* **1906**, *324*, 289−306.
(8) Riseman, J.; Kirkwood, J. G. The intrinsic viscosity, translational and rotatory diffusion constants of rod-like macromolecules in solution. *J. Chem. Phys.* **1950**, *18*, 512−516.
(9) Lin, C. C.; Parrish, E.; Composto, R. J. Macromolecule and particle dynamics in confined media. *Macromolecules* **2016**, *49*, 5755−5772.
(10) Choi, J.; Cargnello, M.; Murray, C. B.; Clarke, N.; Winey, K. I.; Composto, R. J. Fast nanorod diffusion through entangled polymer melts. *ACS Macro Lett.* **2015**, *4*, 952−956.
(11) Yamamoto, U.; Carrillo, J. M. Y.; Bocharova, V.; Sokolov, A. P.; Sumpter, B. G.; Schweizer, K. S. Theory and simulation of attractive nanoparticle transport in polymer melts. *Macromolecules* **2018**, *51*, 2258−2267.
(12) Yamamoto, U.; Schweizer, K. S. Spatially dependent relative diffusion of nanoparticles in polymer melts. *J. Chem. Phys.* **2013**, *139*, 064907.
(13) Yamamoto, U.; Schweizer, K. S. Theory of nanoparticle diffusion in unentangled and entangled polymer melts. *J. Chem. Phys.* **2011**, *135*, 224902.
(14) Yamamoto, U.; Schweizer, K. S. Theory of entanglements and tube confinement in rod-sphere nanocomposites. *ACS Macro Lett.* **2013**, *2*, 955.
(15) Yamamoto, U.; Schweizer, K. S. Microscopic theory of the long-time diffusivity and intermediate-time anomalous transport of a nanoparticle in polymer melts. *Macromolecules* **2015**, *48*, 152.
(16) Yamamoto, U.; Schweizer, K. S. Microscopic theory of the effect of spherical obstacles on the diffusion of topologically entangled needle fluids. *ACS Macro Lett.* **2015**, *4*, 53.
(17) Rudyak, V. Y.; Krasnolutskii, S. L.; Ivanov, D. A. Molecular dynamics simulation of nanoparticle diffusion in dense fluids. *Microfluid. Nanofluid.* **2011**, *11*, 501−506.
(18) Zhang, K.; Kumar, S. K. Molecular simulations of solute transport in polymer melts. *ACS Macro Lett.* **2017**, *6*, 864−868.
(19) Karatrantos, A.; Composto, R. J.; Winey, K. I.; Clarke, N. Polymer and spherical nanoparticle diffusion in nanocomposites. *J. Chem. Phys.* **2017**, *146*, 203331.
(20) Bernardo, G.; Choudhury, R. P.; Beckham, H. W. Diffusivity of small molecules in polymers: Carboxylic acids in polystyrene. *Polymer* **2012**, *53*, 976−983.
(21) Bernardo, G. Diffusivity of alcohols in amorphous polystyrene. *J. Appl. Polym. Sci.* **2013**, *127*, 1803−1811.
(22) Kalathi, J. T.; Yamamoto, U.; Schweizer, K. S.; Grest, G. S.; Kumar, S. K. Nanoparticle diffusion in polymer nanocomposites. *Phys. Rev. Lett.* **2014**, *112*, 108301.
(23) de Gennes, P. G. Motions of one stiff molecule in an entangled polymer melt. *J. Phys. (Paris)* **1981**, *42*, 473−477.
(24) Wyart, F. B.; de Gennes, P. G. Viscosity at small scales in polymer melts. *Eur. Phys. J. E: Soft Matter Biol. Phys.* **2000**, *1*, 93−97.
(25) Lee, J.; Grein-Iankovski, A.; Narayanan, S.; Leheny, R. L. Nanorod mobility within entangled wormlike micelle solutions. *Macromolecules* **2017**, *50*, 406−415.
(26) Cai, L. H.; Panyukov, S.; Rubinstein, M. Hopping diffusion of nanoparticles in polymer matrices. *Macromolecules* **2015**, *48*, 847−862.
(27) Kohli, I.; Mukhopadhyay, A. Diffusion of nanoparticles in semidilute polymer solutions: effect of different length scales. *Macromolecules* **2012**, *45*, 6143−6149.
(28) Nath, P.; Mangal, R.; Kohle, F. F. E.; Choudhury, S.; Narayanan, S.; Wiesner, U. B.; Archer, L. A. Dynamics of nanoparticles in entangled polymer solutions. *Langmuir* **2018**, *34*, 241−249.
(29) Senanayake, K. K.; Fakhrabadi, E. A.; Liberatore, M. W.; Mukhopadhyay, A. Diffusion of nanoparticles in entangled poly(vinyl alcohol) solutions and gels. *Macromolecules* **2019**, *52*, 787.
(30) Molaei, M.; Atefi, E.; Crocker, J. C. Nanoscale rheology and anisotropic diffusion using single gold nanorod probes. *Phys. Rev. Lett.* **2018**, *120*, 118002.
(31) Kim, J. M.; Cho, H. W.; Kim, J.; Kim, H.; Sung, B. J. Translational and rotational diffusion of a single nanorod in unentangled polymer melts. *Phys. Rev. E* **2015**, *92*, 042601.
(32) Li, J.; Ding, M.; Zhang, R.; Shi, T. Effects of surface roughness on self-diffusion dynamics of single polymer. *Soft Matter* **2018**, *14*, 3550−3556.
(33) Alam, S.; Mukhopadhyay, A. Translational anisotropy and rotational diffusion of gold nanorods in colloidal sphere solutions. *Langmuir* **2015**, *31*, 8780−8785.
(34) Brouzet, C.; Mittal, N.; Söderberg, L. D.; Lundell, F. Size-dependent orientational dynamics of brownian nanorods. *ACS Macro Lett.* **2018**, *7*, 1022−1027.
(35) Xue, C.; Zheng, X.; Chen, K.; Tian, Y.; Hu, G. Probing non-gaussianity in confined diffusion of nanoparticles. *J. Phys. Chem. Lett.* **2016**, *7*, 514−519.
(36) Parrish, E.; Caporizzo, M. A.; Composto, R. J. Network confinement and heterogeneity slows nanoparticle diffusion in polymer gels. *J. Chem. Phys.* **2017**, *146*, 203318.
(37) Patti, A. Molecular dynamics of spherical nanoparticles in dense polymer melts. *J. Phys. Chem. B* **2014**, *118*, 3731−3742.
(38) Zhang, K.; Meng, D.; Muller-Plathe, F.; Kumar, S. K. Coarse-grained molecular dynamics simulation of activated penetrant transport in glassy polymers. *Soft Matter* **2018**, *14*, 440.
(39) Karatrantos, A.; Koutsawa, Y.; Dubois, P.; Clarke, N.; Kroger, M. Miscibility and diffusion in ionic nanocomposites. *Polymers* **2018**, *10*, 1010.
(40) Kumar, S. K.; Szamel, G.; Douglas, J. F. Nature of the breakdown in the stokes-einstein relationship in a hard sphere fluid. *J. Chem. Phys.* **2006**, *124*, 214501.
(41) Zhao, J.; Wu, L.; Zhan, C.; Shao, Q.; Guo, Z.; Zhang, L. Overview of polymer nanocomposites: Computer simulation understanding of physical properties. *Polymer* **2017**, *133*, 272.
(42) Karatrantos, A.; Clarke, N.; Kröger, M. Modeling of polymer structure and conformations in polymer nanocomposites from atomistic to mesoscale: A review. *Polym. Rev.* **2016**, *56*, 385−428.
(43) Karatrantos, A.; Composto, R. J.; Winey, K. I.; Clarke, N. Primitive path network, structure and dynamics of SWCNT/polymer nanocomposites. *IOP Conf. Ser.: Mater. Sci. Eng.* **2012**, *40*, 012027.
(44) Cheng, S.; Xie, S. J.; Carrillo, J. M. Y.; Carroll, B.; Martin, H.; Cao, P. F.; Dadmun, M. D.; Sumpter, B. G.; Novikov, V. N.; Schweizer, K. S.; Sokolov, A. P. Big effect of small nanoparticles: A shift in paradigm for polymer nanocomposites. *ACS Nano* **2017**, *11*, 752−759.
(45) Bekker, H.; Berendsen, H. J. C.; Dijkstra, E. J.; Achterop, S.; van Drunen, R.; van der Spoel, D.; Sijbers, A.; Keegstra, H.; Reitsma, B.; Renardus, M. K. R. Gromacs: A parallel computer for molecular dynamics simulations. *Phys. Comput.* **1993**, *92*, 252.
(46) Berendsen, H. J. C.; van der Spoel, D.; van Drunen, R. Gromacs: A message-passing parallel molecular dynamics implementation. *Comput. Phys. Commun.* **1995**, *91*, 43−56.
(47) Lindahl, E.; Hess, B.; van der Spoel, D. Gromacs 3.0: A package for molecular simulation and trajectory analysis. *J. Mol. Model.* **2001**, *7*, 306−317.

DOI: 10.1021/acs.macromol.8b02141
Macromolecules XXXX, XXX, XXX−XXX

(48) van der Spoel, D.; Lindahl, E.; Hess, B.; Groenhof, G.; Mark, A. E.; Berendsen, H. J. C. Gromacs: Fast, flexible and free. *J. Comput. Chem.* **2005**, *26*, 1701−1718.
(49) Kremer, K.; Grest, G. S. Dynamics of entangled linear polymer melts: A molecular-dynamics simulation. *J. Chem. Phys.* **1990**, *92*, 5057.
(50) Bulacu, M.; van der Giessen, E. Effect of bending and torsion rigidity on self-diffusion in polymer melts: A molecular-dynamics study. *J. Chem. Phys.* **2005**, *123*, 114901.
(51) Hoy, R. S.; Foteinopoulou, K.; Kröger, M. Topological analysis of polymeric melts: Chain-length effects and fast-converging estimators for entanglement length. *Phys. Rev. E* **2009**, *80*, 031803.
(52) Kröger, M. Shortest multiple disconnected path for the analysis of entanglements in two- and three-dimensional polymeric systems. *Comput. Phys. Commun.* **2005**, *168*, 209−232.
(53) Allen, M. P.; Tildesley, D. J. *Computer Simulation of Liquids*; Clarendon Press: Oxford, 1987.
(54) Auhl, R.; Everaers, R.; Grest, G. S.; Kremer, K.; Plimpton, S. J. Equilibration of long chain polymer melts in computer simulations. *J. Chem. Phys.* **2003**, *119*, 12718.
(55) Hoy, R. S.; Robbins, M. O. Effect of equilibration on primitive path analyses on entangled polymers. *Phys. Review E* **2005**, *72*, 061802.
(56) Li, Y.; Kröger, M.; Liu, W. K. Dynamic structure of unentangled polymer chains in the vicinity of non-attractive nanoparticles. *Soft Matter* **2014**, *10*, 1723−1737.
(57) Hockney, R. W.; Goel, S. P.; Eastwood, J. Quiet high resolution computer models of a plasma. *J. Comput. Phys.* **1974**, *14*, 148−158.
(58) Shen, J.; Li, X.; Zhang, L.; Lin, X.; Li, H.; Shen, X.; Ganesan, V.; Liu, J. Mechanical and viscoelastic properties of polymer-grafted nanorod composites from molecular dynamics simulation. *Macromolecules* **2018**, *51*, 2641−2652.
(59) Chen, Y.; Xu, Q.; Jin, Y.; Qian, X.; Liu, L.; Liu, J.; Ganesan, V. Design of end-to-end assembly of side-grafted nanorods in a homopolymer matrix. *Macromolecules* **2018**, *51*, 4143−4157.
(60) Hore, M. J. A.; Composto, R. J. Strategies for dispersing, assembling, and orienting nanorods in polymers. *Curr. Opin. Chem. Eng.* **2013**, *2*, 95−102.
(61) Sankar, U. K.; Tripathy, M. Dispersion, depletion, and bridging of athermal and attractive nanorods in polymer melt. *Macromolecules* **2015**, *48*, 432−442.
(62) Zhou, Y.; Huang, M.; Lu, T.; Guo, H. Nanorods with different surface properties in directing the compatibilization behavior and the morphological transition of immiscible polymer blends in both shear and shear-free conditions. *Macromolecules* **2018**, *51*, 3135−3148.
(63) Gooneie, A.; Hufenus, r. Hybrid carbon nanoparticles in polymer matrix for efficient connected networks: Self-assembly and continuous pathways. *Macromolecules* **2018**, *51*, 3547−3562.
(64) Golosova, A. A.; Adelsberger, J.; Sepe, A.; Niedermeier, M. A.; Lindner, P.; Funari, S. S.; Jordan, R.; Papadakis, C. M. Dispersions of polymer-modified carbon nanotubes: A small-angle scattering investigation. *J. Phys. Chem. C* **2012**, *116*, 15765−15774.
(65) Gao, Y.; Liu, J.; Shen, J.; Zhang, L.; Cao, D. Molecular dynamics simulation of dispersion and aggregation kinetics of nanorods in polymer nanocomposites. *Polymer* **2014**, *55*, 1273−1281.
(66) Wescott, J. T.; Kung, P.; Maiti, A. Conductivity of carbon nanotube polymer composites. *Appl. Phys. Lett.* **2007**, *90*, 033116.
(67) Gao, Y.; Liu, J.; Shen, J.; Wu, Y.; Zhang, L. Influence of various nanoparticle shapes on the interfacial chain mobility:a molecular dynamics simulation. *Phys. Chem. Chem. Phys.* **2014**, *16*, 21372.
(68) Liu, J.; Wu, Y.; Shen, J.; Gao, Y.; Zhang, L.; Cao, D. Polymer-nanoparticle interfacial behavior revisited: A molecular dynamics study. *Phys. Chem. Chem. Phys.* **2011**, *13*, 13058−13069.
(69) Toepperwein, G. N.; Karayiannis, N. Ch.; Riggleman, R. A.; Kröger, M.; de Pablo, J. J. Influence of nanorod inclusions on structure and primitive path network of polymer nanocomposites at equilibrium and under deformation. *Macromolecules* **2011**, *44*, 1034.
(70) Kröger, M.; Loose, W.; Hess, S. Structural changes and rheology of polymer melts via nonequilibrium molecular dynamics. *J. Rheol.* **1993**, *37*, 1057−1079.
(71) Kalathi, J. T.; Grest, G. S.; Kumar, S. K. Universal viscosity behavior of polymer nanocomposites. *Phys. Rev. Lett.* **2012**, *109*, 198301.
(72) Karatrantos, A. Isotropic - nematic transition and dynamics of rigid charged molecules. *Chem. Phys. Lett.* **2016**, *647*, 89−94.
(73) de Gennes, P. G. Reptation of a polymer chain in the presence of fixed obstacles. *J. Chem. Phys.* **1971**, *55*, 572.
(74) Liu, J.; Cao, D.; Zhang, L. Molecular dynamics study on nanoparticle diffusion in polymer melts: A test of the stokes-einstein law. *J. Phys. Chem. C* **2008**, *112*, 6653−6661.
(75) Volgin, I. G.; Larin, S. V.; Lyulin, A. V.; Lyulin, S. V. Coarse-grained molecular-dynamics simulations of nanoparticle diffusion in polymer nanocomposites. *Polymer* **2018**, *145*, 80−87.
(76) Grabowski, C. A.; Adhikary, B.; Mukhopadhyay, A. Dynamics of gold nanoparticles in a polymer melt. *Appl. Phys. Lett.* **2009**, *94*, 021903.
(77) Grabowski, C. A.; Mukhopadhyay, A. Size effect of nanoparticle diffusion in a polymer melt. *Macromolecules* **2014**, *47*, 7238−7242.
(78) Tuteja, A.; Mackay, M. E.; et al. Breakdown of the continuum stokes-einstein relation for nanoparticle diffusion. *Nano Lett.* **2007**, *7*, 1276−1281.
(79) Egorov, S. A. Anomalous nanoparticle diffusion in polymer solutions and melts: A mode-coupling theory study. *J. Chem. Phys.* **2011**, *134*, 084903.
(80) Ganesan, V.; Pryamitsyn, V.; Surve, M.; Narayanan, B. Noncontinuum effects in nanoparticle dynamics in polymers. *J. Chem. Phys.* **2006**, *124*, 221102.
(81) Ren, K. X.; Jia, X. M.; Jiao, G. S.; Chen, T.; Qian, H. J.; Lu, Z. Y. Interfacial properties and hopping diffusion of small nanoparticle in polymer/nanoparticle composite with attractive interaction on side group. *Polymers* **2018**, *10*, 598.
(82) Kumar, S. K.; Krishnamoorti, R. Nanocomposites: Structure, phase behavior, and properties,. *Annu. Rev. Chem. Biomol. Eng.* **2010**, *1*, 37−58.
(83) Karatrantos, A.; Clarke, N.; Composto, R. J.; Winey, K. I. Topological entanglement length in polymer melts and nano-composites by a DPD polymer model. *Soft Matter* **2013**, *9*, 3877−3884.
(84) Riggleman, R. A.; Toepperwein, G.; Papakonstantopoulos, G. J.; Barrat, J.-L.; de Pablo, J. J. Entanglement network in nanoparticle reinforced polymers. *J. Chem. Phys.* **2009**, *130*, 244903−6.
(85) Karatrantos, A.; Clarke, N.; Composto, R. J.; Winey, K. I. Structure, entanglements and dynamics of polymer nanocomposites containing spherical nanoparticles. *IOP Conf. Ser.: Mater. Sci. Eng.* **2014**, *64*, 012041.
(86) Glomann, T.; Hamm, A.; Allgaier, J.; Hubner, E. G.; Radulescu, A.; Farago, B.; Schneider, G. J. A microscopic view on the large scale chain dynamics in nanocomposites with attractive interactions. *Soft Matter* **2013**, *9*, 10559.
(87) Holt, A. P.; Griffin, P. J.; Bocharova, V.; Agapov, A. L.; Imel, A. E.; Dadmun, M. D.; Sangoro, J. R.; Sokolov, A. P. Dynamics at the polymer/nanoparticle interface in poly(2-vinylpyridine)/silica nano-composites. *Macromolecules* **2014**, *47*, 1837−1843.
(88) Toepperwein, G. N.; Riggleman, R. A.; de Pablo, J. J. Dynamics and deformation response of rod-containing nanocomposites. *Macromolecules* **2012**, *45*, 543−554.
(89) Lin, C. C.; Cargnello, M.; Murray, C. B.; Clarke, N.; Winey, K. I.; Riggleman, R. A.; Composto, R. J. Nanorod mobility influences polymer diffusion in polymer nanocomposites. *ACS Macro Lett.* **2017**, *6*, 869−874.
(90) Mangal, R.; Wen, Y. H.; Choudhury, S.; Archer, L. A. Multiscale dynamics of polymers in particle-rich nanocomposites. *Macromolecules* **2016**, *49*, 5202.
(91) Casalini, R.; Roland, C. M. Local and global dynamics in polypropylene glycol/silica composites. *Macromolecules* **2016**, *49*, 3919−3924.

DOI: 10.1021/acs.macromol.8b02141
Macromolecules XXXX, XXX, XXX−XXX

(92) Kropka, J. M.; Sakai, V. G.; Green, P. F. Local polymer dynamics in polymer-c60 mixtures. *Nano Lett.* **2008**, *8*, 1061−1065.

DOI: 10.1021/acs.macromol.8b02141
Macromolecules XXXX, XXX, XXX−XXX